



pH-Sensitive Nanocomposite Hydrogels Based on Poly(Vinyl Alcohol) Macromonomer and Graphene Oxide for Removal of Cationic Dyes from Aqueous Solutions

Mina Rabipour¹ · Zahra Sekhavat Pour¹ · Razieh Sahraei² · Mousa Ghaemy¹ · Mehdi Erfani Jazi³ · Todd E. Mlsna³

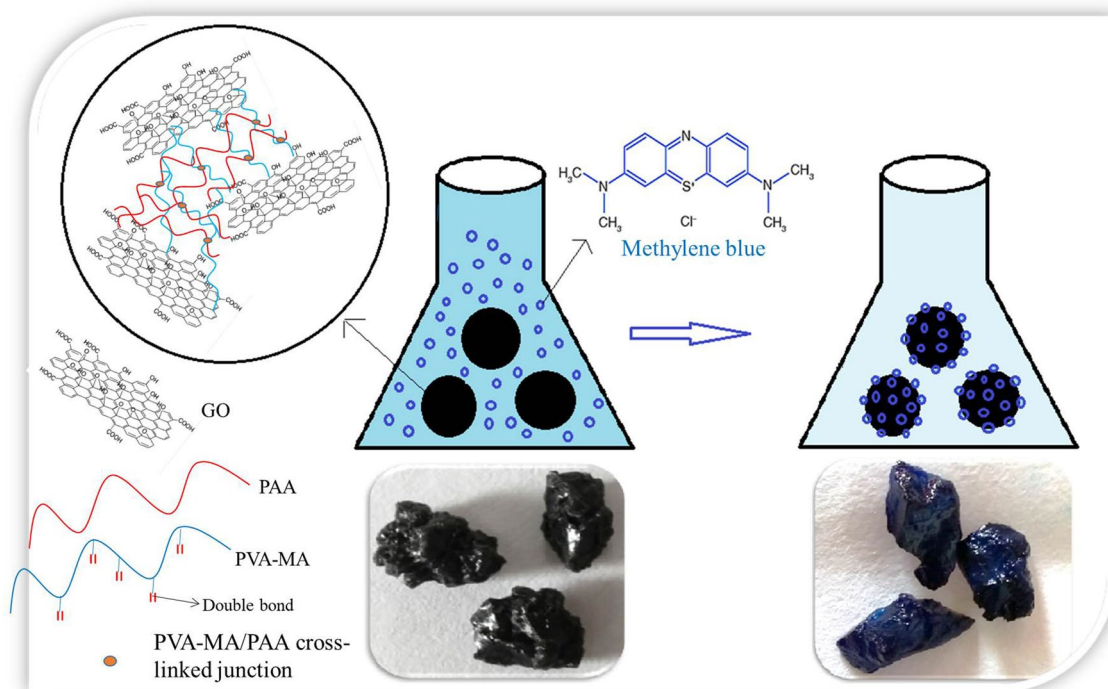
Published online: 9 December 2019

© Springer Science+Business Media, LLC, part of Springer Nature 2019

Abstract

In this study, a pH-sensitive nanocomposite hydrogel based on poly(vinyl alcohol) (PVA)/graphene oxide (GO) was prepared and used as a potential adsorbent for the removal of crystal violet (CV) and methylene blue (MB) from aqueous solutions. The prepared nanocomposite hydrogels were fully characterized and their swelling capacity and gel content were investigated by changing the GO and acrylic acid (AA) content. Adsorption experiments were carried out as a function of contact time, concentration, temperature, pH and dosage. The adsorption process was favored at higher pHs, followed pseudo second-order kinetics while the adsorption equilibrium data well fitted to the Langmuir isotherm model with the maximum capacity of 173.2 and 169.6 mg g⁻¹ for MB and CV, respectively. A thermodynamic study showed the spontaneity nature of the adsorption process for MB and CV. The removal percentage of MB dye increased with increase of temperature from 25 to 55 °C while the adsorption of CV dye showed the opposite trend. This different trend can be attributed to the differences in the pattern of adsorption.

Graphic Abstract



Extended author information available on the last page of the article

Keywords Hydrogel · Nanocomposite · Graphene oxide · Adsorption · Dye

Introduction

The discharge of wastewaters containing dyes from many industries such as textile, dyeing, paper and pulp, tannery and paint into river streams not only harm the aesthetic nature of the environment, but they are also commonly toxic to aquatic life [1]. Cationic dyes can enter into the cells by interacting with the negatively charged cell membrane surface and building up in the cytoplasm causing harmful effects such as heartbeat increase, vomiting, shock, cyanosis, jaundice, quadriplegia, and tissue necrosis in humans [2, 3]. A wide range of methods such as chemical oxidation [4], microbiological or enzymatic decompositions [5], electrochemical treatment [6], etc., have been developed for the removal of synthetic dyes from wastewater. However, due to some limitations existing in these methods; the removal of dye from industrial effluents is a field of research receiving increasing attention. Among these methods, adsorption has been found to be superior for water reuse in terms of initial cost, flexibility and simplicity of design, ease of operation, and insensitivity to toxic pollutants [7]. Adsorption by hydrogels has been the focus of research for environmental scientists due to their characteristic properties such as adsorption-regeneration, economic feasibility, and environmental friendly behavior. The porous structure network of hydrogel and also the presence of ionic functional groups of hydrogels allow solute diffusion and trapping ionic species like dye molecules [8].

Poly(vinyl alcohol) (PVA) has a wide commercial application due to its unique chemical and physical properties. It is a nontoxic, highly crystalline, and water-soluble polymer and has good film forming and high hydrophilic properties. However, PVA as a soluble polymer cannot be used in the treatment of wastewaters. Thus, it has to be converted to a completely insoluble material with high mechanical properties. Reagents such as glutaraldehyde, boric acid, and epichlorohydrin, and methods such as photo-curing technique were used for preparing PVA based hydrogel [9–11]. However, there are few reports for preparing PVA hydrogel based on chemically modified poly(vinyl alcohol).

Graphene oxide (GO), as a reinforcing filler in new composite materials, can be incorporated into the hydrogel structure by various supramolecular interactions including hydrogen bonding, electrostatic interaction, coordination, and π - π stacking [12, 13]. Graphene oxide is expected to be able to significantly improve the swelling property, mechanical strength, and adsorption ability of polymeric hydrogel due to large surface area and hydrophilic polar groups [13, 14].

The objective of this work was to prepare PVA/GO-based pH sensitive nanocomposite hydrogel with high rate

of adsorption for removal of cationic dyes of crystal violet (CV) and methylene blue (MB) from aqueous solution. For this aim, PVA was functionalized with unsaturated carboxylic acid by grafting with maleic anhydride (MA). The MA grafted-PVA and acrylic acid (AA) were used for preparation of hydrogel via radical copolymerization in the presence of GO by using $K_2S_2O_8$ as initiator. PVA matrix was chosen as a host material as it is one of the most promising polymers due to its unique characteristics including ease of availability, safety, and hydrophilicity. The extended layered structure of GO with large surface area and hydrophilic polar groups can increase swelling property, mechanical strength, and adsorption ability of the hydrogels. The prepared nanocomposite hydrogels were characterized by FTIR, thermal gravimetric analysis (TGA) and scanning electron microscopy (SEM) and the effect of GO and AA content on their swelling capacity and gel content were investigated. The effect of experimental conditions such as adsorbent dosage, pH, contact time, initial dye concentration, temperature, and regeneration of the nanocomposite hydrogel based on the consecutive adsorption/desorption cycles were investigated. Moreover, the kinetics and isotherms of the adsorption process were studied.

Experimental

Materials

Analytical grade PVA (98% hydrolyzed) with a molecular weight average of $49,000 \text{ g mol}^{-1}$ was supplied by Aldrich Chemical Company. Acrylic acid (AA) (Fluka) was purified by soaking in activated carbon. *N,N*-dimethylformamide (DMF), potassium persulphate, pyridine, ethanol, and maleic anhydride (MA), from Merck (Germany), were all analytical grade reagents and used as received. Methylene blue (MB) and crystal violet (CV) were purchased from Sigma-Aldrich and used as the adsorbate without further purification. Graphene oxide nanosheets were supplied by US Research Nanomaterials, Inc. (USA), with a purity of 99%. The thickness of GO nanosheets was 3.4–7 nm.

Synthesis of PVA-Based Macromonomer

To prepare PVA-based macromonomer, 1 g PVA was dissolved in 10 mL *N,N*-dimethylformamide (DMF) in a 50 mL flask at 80 °C for 2 h stirring. A certain amount of maleic anhydride (4 g) was dissolved in 6 mL DMF, and mixed with pyridine as catalyst. The solution of maleic anhydride was added into the flask in droplet under stirring at 30 °C

under N₂ atmosphere and then stirred vigorously for 24 h. The crude product was precipitated from 95% ethanol and purified by washing with ethanol for three times. The dried light yellow powder was pure macromonomer (PVA-MA).

Synthesis of PVA-Based Nanocomposite Hydrogel

To prepare the PVA-based nanocomposite hydrogel, 0.25 g macromonomer was dissolved in 5 mL distilled water at 70 °C. A certain amount of graphene oxide was dispersed in distilled water ultrasonically and added to the above solution. The polymerization initiated with potassium persulfate and reacted with a predetermined amount of acrylic acid under N₂ atmosphere for 24 h. Five hydrogels with different amounts of components were prepared as listed in Table 1.

Characterizations

FT-IR spectra were recorded on KBr pellet using a Bruker Vector 22 FTIR spectrophotometer in the range of 400–4000 cm⁻¹. ¹H NMR (400 MHz) spectra of PVA-MA macromonomer was obtained on a Bruker DRX 400 Advance spectrometer at room temperature with D₂O as solvent and tetramethylsilane (TMS) as the internal standard. Chemical shifts are reported in ppm relative to the deuterated solvent resonances.

The surface morphology of hydrogels was investigated by using scanning electron microscopy (SEM) (Model: Hitachi S4160). Before the investigation, all the samples were coated with gold. Thermogravimetric analysis of PVA, the PVA-MA macromonomer and hydrogels were performed with a TAV2.4F thermoanalyzer, which was conducted over the temperature range from 25 to 600 °C with a rate of 10 °C min⁻¹ under nitrogen atmosphere.

To measure the gel content (%) of the prepared samples, freshly prepared hydrogels were dried in a vacuum oven at 50 °C to a constant weight (*W*₀). The dried gels were soaked in distilled water for 48 h in 70 °C to remove the sol fraction. Then, the gels were dried again to a constant weight (*W*_{*t*}). The gel fraction (%) was calculated using Eq. (1).

$$\text{Gel content (\%)} = \frac{W_1}{W_0} \times 100 \quad (1)$$

The swelling studies of prepared hydrogel were carried out in distilled water at room temperature by a gravimetric method. To measure the swelling percent, the clean and dried hydrogels were weighted and immersed in distilled water at room temperature. At regular time intervals, the samples were removed from the medium, and the swollen samples were then weighted at predetermined time till the weights reached swelling balance. The swelling ratio was calculated by using the Eq. (2):

$$\text{Swelling (\%)} = \frac{W_t - W_0}{W_0} \times 100 \quad (2)$$

where *W*₀ and *W*_{*t*} are the weights of the original dry sample and the weights of swollen hydrogels at time *t*, respectively.

Dye Adsorption

The adsorption studies were performed by batch equilibration method. The CV and MB solutions for adsorption experiments were prepared via serial dilution of their stock solution (1000 mg L⁻¹) to desired concentrations. For studying the effect of sorbent dosage, a certain amount of sorbent (2–50 mg) was added to 25 mL of known concentration of CV or MB solution in a beaker and stirred for 24 h at room temperature and a fixed pH. After adsorption equilibrium was achieved, the supernatant was separated from the sorbent by centrifugation and the concentration of dye in supernatant was analyzed with a UV-Vis spectrophotometer at a wavelength of 590 nm, maximum absorbance, for CV and 664 nm for MB. The removal percentage (*R*, %) and the adsorption capacity (*Q*_{*e*}, mg g⁻¹) of the hydrogels were calculated as follows (Eqs. (3) and (4)):

$$R(\%) = \frac{C_0 - C_e}{C_0} \times 100 \quad (3)$$

$$Q_e = \frac{(C_0 - C_e)V}{m} \quad (4)$$

where *C*₀ and *C*_{*e*} (mg L⁻¹) are the concentrations of dye in initial solution and in aqueous phase after adsorption, respectively, *m* is the weight of sorbent and *V* is the volume of dye solutions (L).

The influence of solution pH values on dye removal was also studied by adding defined amount of the adsorbents into the beaker containing 25 mL of different dye solution with pH values ranging from 2 to 12. The pH of the initial solution was adjusted to the required pH value using either 0.1 M HNO₃ or 0.1 M NaOH. Dye adsorption isotherms were determined with a constant dosage of sorbent, in which

Table 1 Feed composition for hydrogel synthesis

Hydrogel	Feed (g)		Equilibrium swelling ratio (%)	Gel content (%)
	AA	GO		
PAH	2	0	90.4	94
GPAH1	0.5	5	123.1	89
GPAH2	1	5	135	86
GPAH3	2	5	143.5	84
GPAH4	2	10	178.4	78

at initial concentrations of cationic dyes were varied from 20 to 200 mg L⁻¹. Adsorption kinetics was studied at a constant concentration with changing the contact time in the range of 0.5–24 h. The effect of temperature on sorption was also determined at 25, 35, 45 and 55 °C.

Desorption and Reuse of Regenerated Sorbents

Experiments were conducted in order to assess the regeneration properties of the synthesized GPAH nanocomposite. Desorption of CV adsorbed GPAH nanocomposite was carried out in 25 mL ethanol for 24 h at room temperature while desorption of MB was investigated in 0.1 M NaOH solution. After removal of GPAH from desorption medium, the hydrogel nanocomposite was washed with distilled water and dried at 60 °C and used for the subsequent runs. The adsorption–desorption cycle was repeated four times using the same adsorbents.

Results and Discussion

Characterization of GPAH Nanocomposites

PVA/maleic anhydride (MA) macromonomer, PVA-MA, was prepared via esterification reaction in the presence of pyridine. Then GPAH nanocomposite hydrogel was prepared via radical copolymerization using PVA-MA macromonomer and acrylic acid (AA) in the presence of GO. The detailed mechanistic scheme of synthesis of PVA-based nanocomposite hydrogel is shown in Fig. 1.

The FTIR spectra of PVA-MA and GPAH4 were presented in Fig. 2a. In the FTIR spectrum of PVA, the absorption band at 1097, 1377, and 1730 cm⁻¹ are due to C–O stretching in C–O–H, C–H bending, and the residual acetate groups, respectively. The bands at 2920 and 3409 cm⁻¹ are attributed to C–H stretching and –OH stretching, respectively. Compared with the FTIR spectra of PVA, characteristic absorption band at 1683 cm⁻¹ in the spectrum of PVA-based macromonomer (PVA-MA) is due to the stretching vibration of carboxylate group. The absorption bands at 3092 and 3140 cm⁻¹ are also attributed to the C=C–H vibration and demonstrated the esterification of PVA with maleic anhydride.

The structure of PVA-MA is also confirmed by ¹H NMR (Fig. 2b). According to Fig. 2b the protons of PVA backbone, –CH attached to functional group and the protons of –CH₂, appeared at 3.85 ppm, and 1.40 to 1.90 ppm respectively. There is a distinctive peak in the double bond region (6.3 ppm.) that correlate with the –CH=CH– proton of MA. Graphene oxide (GO) is a nontoxic, bio compatible, and hydrophilic material with high surface area and good chemical stability which can be obtained by treating graphite with

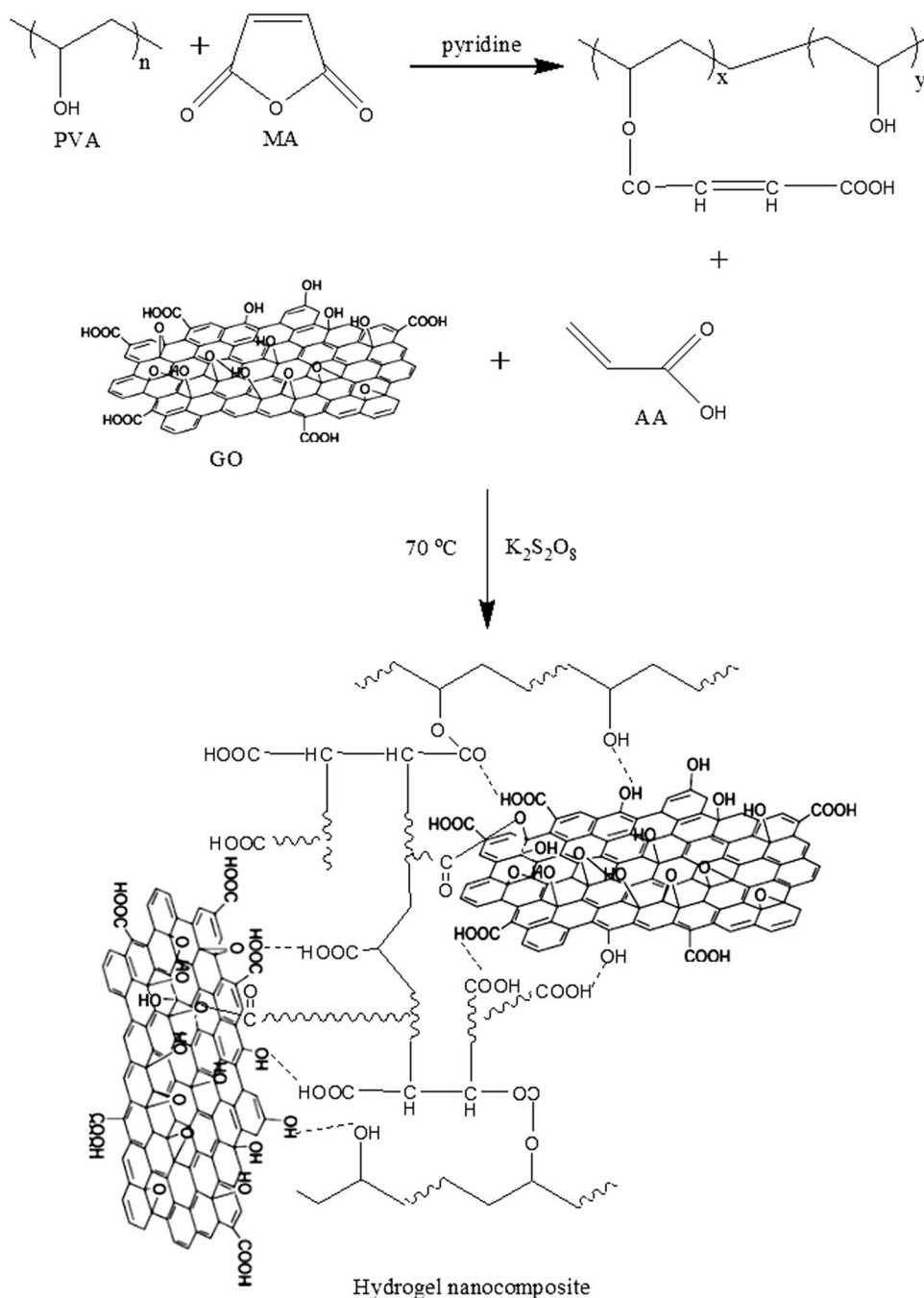
strong oxidants and has been extensively used in materials reinforcement. The presence of various hydrophilic oxygenated functional groups such as epoxy, hydroxyl, and carboxyl on the GO sheets improve swelling and adsorption properties of composite hydrogels. The spectrum of GO demonstrates the characteristic oxygen-containing groups such as: O–H stretching vibration at 3428 cm⁻¹, C=O stretching vibration at 1710 cm⁻¹, unoxidized sp² C=C stretching vibration at 1629 cm⁻¹, O–H bending vibration at 1400 cm⁻¹ and C–O stretching at 1053 cm⁻¹ [15, 16]. The prominent absorption bands of macromonomer, PVA-MA, and GO appeared in the FT-IR spectrum confirmed that GPAH nanocomposite has been successfully synthesized.

GO-based composite hydrogels can be prepared by embedding GO sheets in the network structure of hydrogels via various interactions such as hydrogen bonding, electrostatic interaction, π – π stacking, van der Waals interactions and coordination. The swelling of hydrogels has been studied by researchers to evaluate the water-holding capacity. Hydrogel swelling process can be affected by many factors such as hydrophilicity and hydrophobicity of the materials, and crosslinking and ionization degrees [17]. The swelling of PVA-based adsorbent hydrogel (PAH) and its GO nanocomposite hydrogels (GPAHs) containing different amounts of GO sheets and various feeding percentage of acrylic acid was studied by soaking the samples in deionized water at room temperature, the results are shown in Fig. 3a.

The hydrogels have a similar swelling trend in distilled water. For all samples, swelling increases with time up to a certain level initially, and then it begins to level off and reach equilibrium after about 2 h. Together with the weight gain of the sample during the swelling experiments, noticeable increase in the volume of the sample was also observed. It can be observed in Fig. 3a that when GO is incorporated, the swelling ratio increased and higher amounts of GO cause higher increase in swelling (comparing PAH, GPAH3 and GPAH4).

Compared with the swelling percentage of PAH, 90.4%, the nanocomposites containing only 5 mg GO sheets (GPAH3) acquired more swelling percentage, 143.5% in distilled water. The significant improvement of the swelling of the nanocomposites containing low GO content might be mainly due to plenty of polar groups such as –COOH, –C=O and –C–O–C– groups on the surface of GO sheets which increase the hydrophilicity and facilitate the water diffusion, thus leading to enhanced swelling ratio. However, the crosslinking density of hydrogel might be affected by the GO loading. Since the gel fraction of GPAHs is lower than the PAH, it can be concluded that the crosslinking density in GPAHs is lower due to the GO loading, which restricted interaction between PVA macromonomer and acrylic acid. The swelling ratio and gel fraction of the hydrogels also depend on the amounts of AA and PVA-MA. Hydrogels

Fig. 1 synthesis of PVA-based nanocomposite hydrogel



of higher crosslinking degree absorbs less water and contains fewer water-soluble components, which leads to lower swelling percent and higher gel fraction. According to the obtained data in Table 1, increasing the amount of AA in the constant weight of PVA-MA led to higher swelling percent and lower gel fraction of GPAH (compare GPAH1, GPAH2 and GPAH3). This could be due to an increase in the hydrophilic groups ($-COOH$) and decrease of crosslinking density as a result of reduction of unsaturated $C=C$ bonds of PVA-MA in the polymerization media with increasing the amount of acrylic acid in the feed.

Figure 3b depicts the effect of pH on the swelling percent of GPAH4. As seen in this figure, the prepared hydrogel shows pH-sensitive swelling behavior because of significant increase of swelling with increase of pH from 2 to 13. At a low pH, (pH 2), the formation of physical cross-links due to hydrogen bonding with the AA and other components in the polymer network causes contraction of the hydrogel and less hydrophilicity, resulting in a low swelling rate. As the pH increases, the hydrogen bonds dissociate, the carboxylic acid groups deionize and are charged negatively. The ionic repulsive forces expand

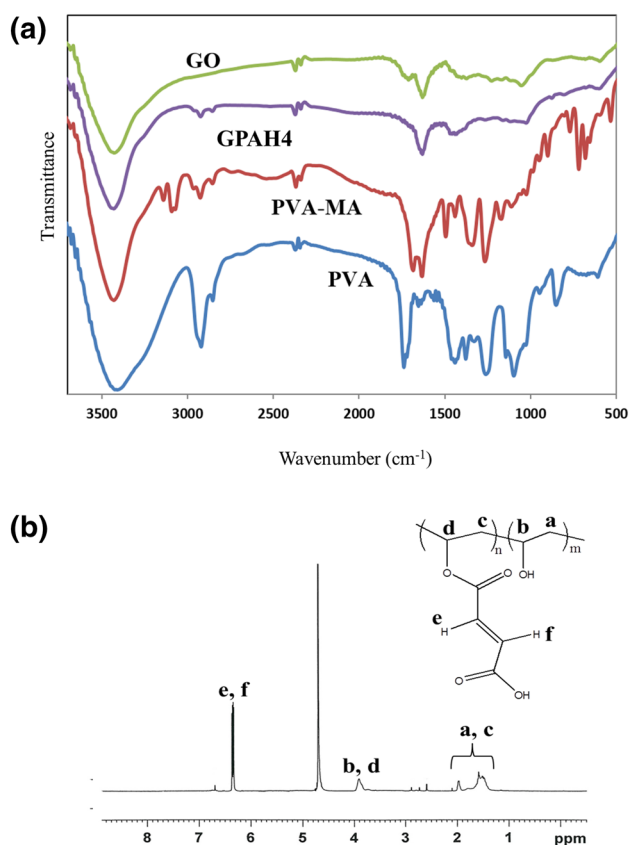


Fig. 2 a FTIR spectra of PVA, GO, PVA-MA and GPAH4, b ^1H NMR of PVA-MA

the coiled conformation of polymer chains, resulting a significant increase in the swelling.

Figure 4 shows the TGA curves of PVA, PVA-MA macromonomer, PAH hydrogel and the nanocomposites. As shown in this figure, the remained fractions of PVA, the PVA-MA and the hydrogels are 8, 3 and ~20 wt% at 600 °C, respectively. This order is consistent with the microstructure of the samples.

PVA showed about 5% weight loss at roughly 100 °C due to evaporation of the adsorbed moisture. The significant weight loss for PVA occurs above 350 °C. This is mainly because the crystallinity in PVA is higher than the crystallinity in PVA-MA macromonomer and the hydrogels. Ring opening reaction of maleic anhydride with the hydroxyl groups of PVA decreases the degree of crystallinity in PVA-MA due to the disturbance of hydrogen bonds between the PVA chains [11]. On the other hand, thermal stability of PAH hydrogel is higher than thermal stability of PVA-MA. It is the cross-linked structure that greatly improves the thermal stability of the hydrogels. However, GO nanocomposites showed slightly higher thermal stability than PAH hydrogel which can be due to the interaction of hydrophilic groups of GO and PAH

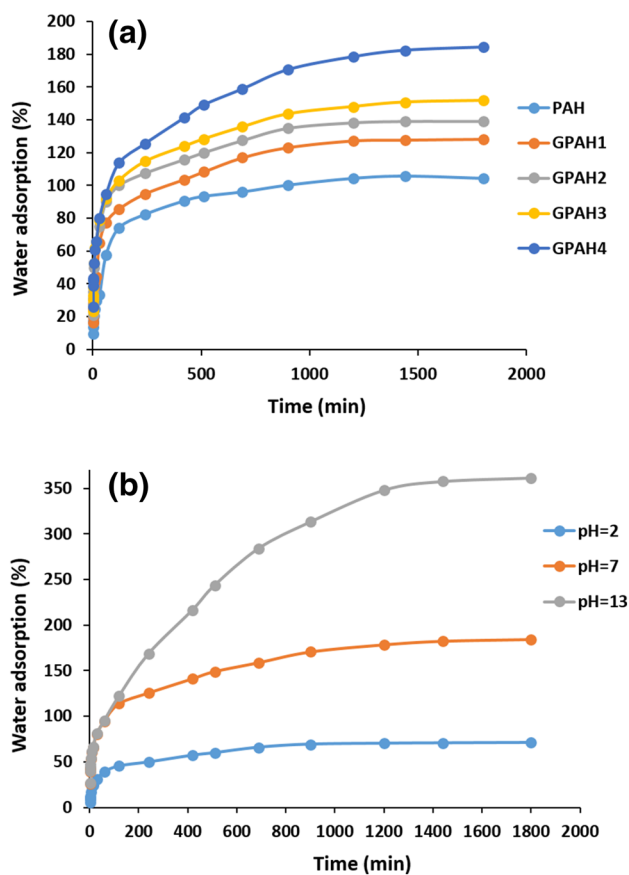


Fig. 3 a Swelling of PAH and nanocomposite hydrogels (GPAHs) in deionized water at room temperature and b effect of pH on the water adsorption of GPAH4

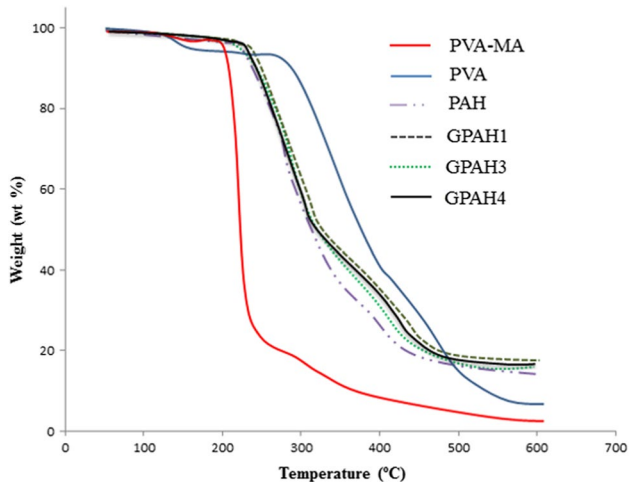


Fig. 4 TGA curves of PVA, PVA-MA, PAH hydrogel and nanocomposites

structure and the barrier effect of GO sheets which retards the volatilization of polymer decomposition [18]. The higher thermal stability of GPAH1 confirmed the higher crosslinking degree of this nanocomposite as estimated by the swelling degree and gel content at earlier paragraph.

Figure 5 shows the SEM images of the dried PAH and GPAH4 nanocomposites. It is clearly seen that the surface morphology of the hydrogel was significantly affected by incorporating of GO nanosheets. The PAH image has an ordinary and almost smooth surface structure (Fig. 5a, b). Obviously the surface of the nanocomposite is very rough compared with the surface of PAH hydrogel. When GO is added, the hydrogel surface becomes stiff and more compact indicating that GO sheets are dispersed homogeneously in the polymer matrix and there are interfacial interactions between GO and the polymer matrix (Fig. 5c, d) [17].

Dye Adsorption Study

Effect of Adsorbent Dosage

The effect of the prepared hydrogel dosage on the adsorption performance of the CV and MB was investigated by immersing certain amount of hydrogels into 25 mL of the dye solutions at the initial concentration of 20 mg/L for 24 h. It can be seen from Fig. 6a, b that the removal percentage, (R %), of CV and MB dyes increased sharply when the amount of PAH and nanocomposite hydrogels (GPAH1 to 4) increased from 2 mg to 10 mg. However, the adsorption of MB and CV reached the equilibrium values (98%) when the amount of adsorbents (GPAH2, GPAH3, and GPAH4) were above 10 mg, while it was still increasing for PAH and GPAH1 adsorbents up to 50 mg. The adsorption capacity (amount of adsorption per unit amount of the hydrogel, Q_e (mg g⁻¹) reduced with increasing the dosage of hydrogels. Therefore, the adsorption percentage (R %) of dyes increased and the

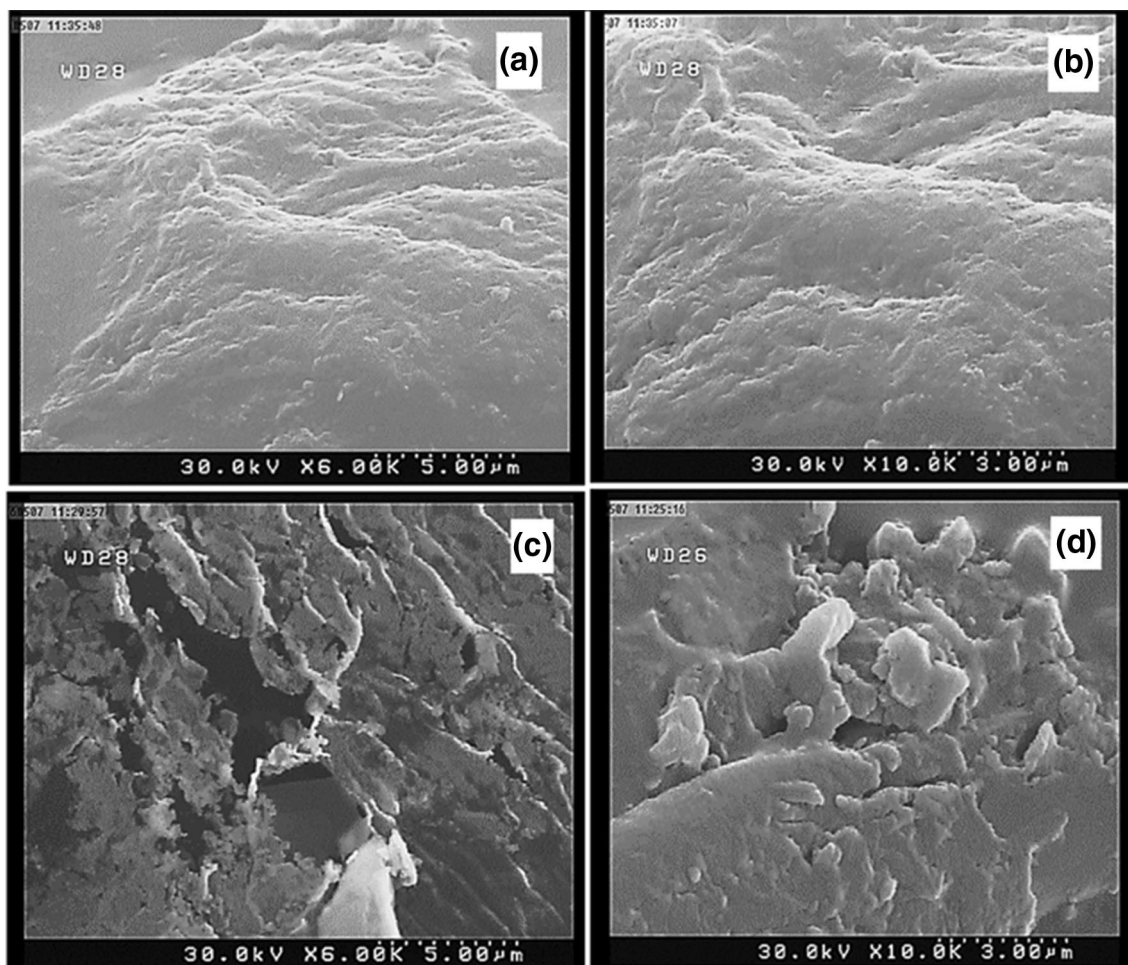


Fig. 5 SEM images of a, b dried PAH and c, d GPAH4 nanocomposites

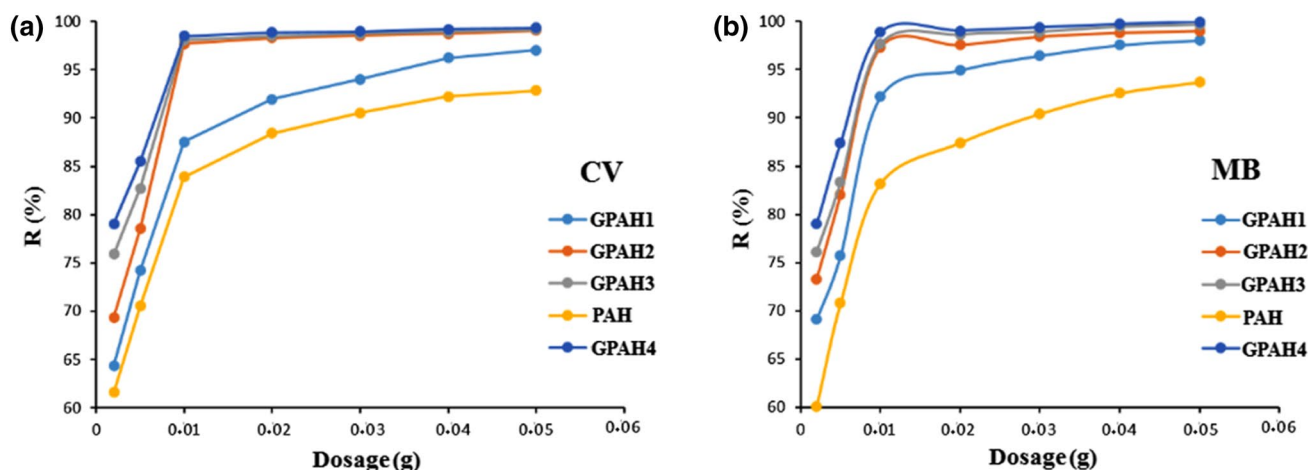


Fig. 6 Effect of adsorbent dosage on the adsorption of **a** CV and **b** MB dyes

adsorption capacity (Q_e , mg g^{-1}) decreased with increasing adsorbent dosage.

This phenomenon is attributed to the presence of greater surface area and more binding sites on the surface of adsorbents forming complex with the dye molecules with increasing the adsorbent dosage leading to the increased removal percentage. However, the total amounts (the initial concentration) of CV and MB are kept constant in this system leading to a decrease in Q_e . Among the prepared hydrogels, GPAH4 nanocomposite showed the highest adsorption for CV and MB dyes and was selected as a sorbent for further experiments. This sample also showed the highest swelling as discussed earlier.

Effect of Initial pH

The pH of the initial dye solution is an important factor in adsorption process. This behavior arises from the effect of ionization degree of the dye molecules and the surface charge of the adsorbent due to the changes in the pH of the solution. The results of the effect of pH (from 2 to 12) on the adsorption of CV and MB (initial concentration 20 mg/L) by the adsorbent GPAH4 (20 mg) for a period of 24 h contact are shown in Fig. 7a. It was observed that the adsorption percentage (R %) of CV and MB increased sharply with increasing pH value from 2 to 7 and reached the maximum values of 99%, then the adsorption remained constant with further increase of pH. The oxygen containing functional groups specially the carboxyl groups in the hydrogel were the groups that affected the adsorption capability [19]. At low pH values, the active groups of GPAH4 nanocomposite such as $-\text{OH}$ and $-\text{COO}^-$ of are protonated. In this condition, adsorption of H^+ ions competes with the adsorption of cationic dyes for the adsorption sites, thus reducing the number of active sites available to interact with dye molecules.

However, by increasing the pH, the carboxyl groups in the hydrogel adsorbent dissociates into $-\text{COO}^-$, and the surface of the adsorbent became negatively charged which would increase the electrostatic attraction between the adsorbent and cationic dye molecule.

Effect of Contact Time (Kinetics Studies)

The contact time between adsorbent and adsorbate is an important factor for understanding the adsorption mechanism because it can control the adsorption kinetics for a given initial concentration of adsorbent [20]. The effect of contact time on the adsorption ability of GPAH4 nanocomposite (20 mg) was investigated using CV and MB (initial concentration 20 mg/L) as model dyes at pH 7 in 25 mL aqueous solution, the results are shown in Fig. 7b. The adsorption curves of CV and MB can be divided into two stages: an initial rapid adsorption within a short time and next a slow adsorption process. The equilibrium adsorption amount is attained after about 7 h for both CV and MB dyes. The abundant active sites (the carboxylate anions $-\text{COO}^-$) of GPAH4 are related to the fast rates of adsorption in the initial period, while the gradual occupation of the active site by dye molecules causes the adsorption rates to slow down. Similar behavior had been reported in the studies of the adsorption of CV on the kappa-carrageenan/poly(vinyl alcohol)/montmorillonite nanocomposite hydrogels [21], and adsorption of MB on the xylan/poly(acrylic acid) magnetic nanocomposite hydrogel [22]. It can be seen that CV and MB are approximately removed from aqueous solution by this hydrogel within 7 h, finally leaving the clear supernatant.

To investigate the adsorption process and potential rate controlling step, the three kinetics models including the pseudo-first-order kinetic model (Eq. (5)), the

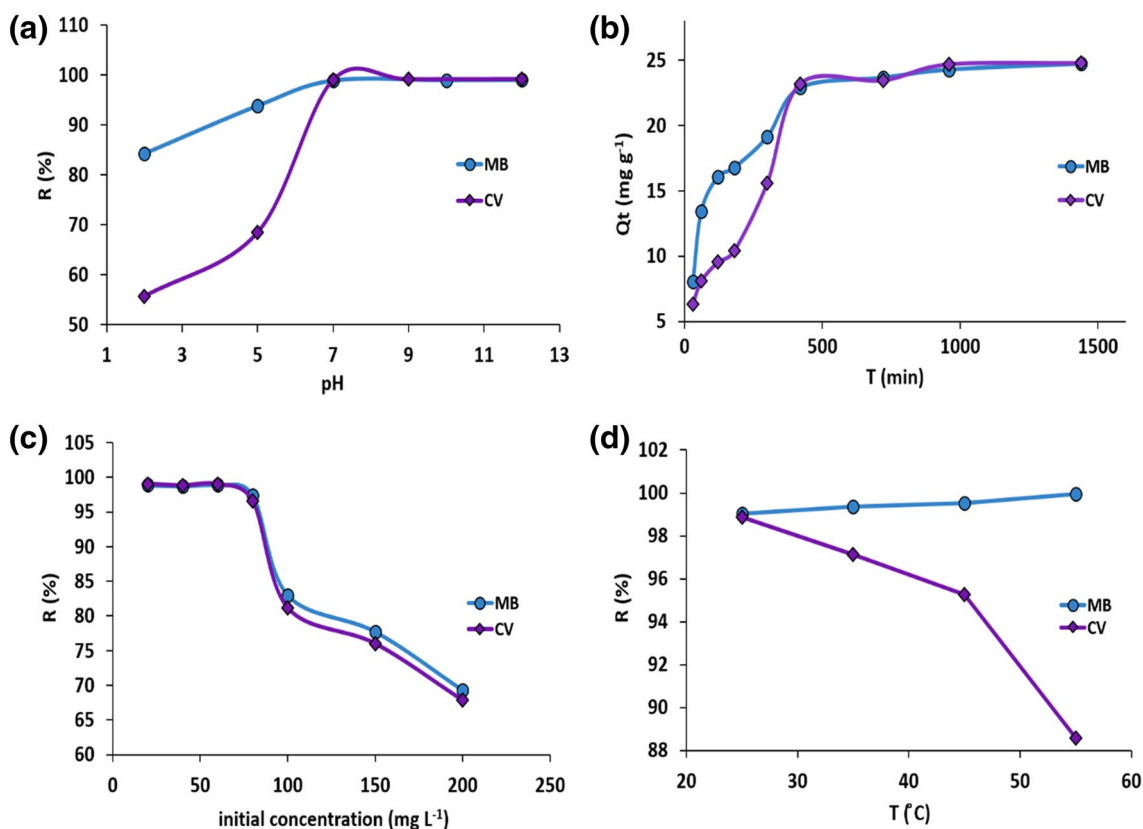


Fig. 7 Effect of **a** pH, **b** contact time, **c** initial concentration of tested dyes and **d** temperature on the adsorption of CV and MB dyes by GPAH4

pseudo-second-order kinetic model (Eq. (6)), and intra-particle diffusion model (Eq. (7)) were applied to fit the obtained experimental data. Listed models are respectively presented by the following equations:

$$\log(Q_e - Q_t) = \log Q_e - \frac{K_1 t}{2.303} \quad (5)$$

$$\frac{t}{Q_t} = \frac{1}{K_2 Q_e^2} + \frac{1}{Q_e} t \quad (6)$$

$$Q_t = k_{id} t^{0.5} + C \quad (7)$$

here the Q_e and Q_t are the adsorption capacity (mg g⁻¹) on the hydrogel at the equilibrium and at time t , respectively; K_1 (min⁻¹) and K_2 (g mg⁻¹ min⁻¹) are the rate constants of the pseudo-first order and the pseudo-second order adsorption, respectively, which can be obtained from $\log(Q_e - Q_t)$ versus t and t/Q_t versus t , respectively, and C is intercept (mg g⁻¹) and k_{id} (mg g⁻¹ min^{-1.5}) is the Intra-particle diffusion rate constant, which can be evaluated from the slop of the linear plot of Q_t versus $t^{0.5}$ [10, 23].

The results of adsorption kinetics (obtained kinetic parameters and correlation coefficients (R^2)) of GPAH4

to CV and MB are shown in Table 2. The fits of experimental kinetic data to the above-mentioned models were evaluated by R^2 . According to Table 2, the R^2 values for pseudo-second order model were found to be higher and much closer to unity (for MB $R^2 = 0.9987$ and for CV $R^2 = 0.9776$) than those for the pseudo-first order model (for MB $R^2 = 0.9672$ and for CV $R^2 = 0.9293$); as a result, the adsorption kinetics of CV and MB onto GPAH4

Table 2 Kinetic parameters of CV and MB dye adsorption onto GPAH4 nanocomposite

Kinetic model	Parameters	CV	MB
Pseudo-first-order	$Q_{e1, cal}$ (mg g ⁻¹)	27.848	14.73
	K_1 (min ⁻¹)	0.005	0.0037
	R^2	0.9293	0.9672
Pseudo-second-order	$Q_{e2, cal}$ (mg g ⁻¹)	27.57	26.042
	$Q_{e, exp}$ (mg g ⁻¹)	24.759	24.715
	K_2 (g mg ⁻¹ min ⁻¹)	0.0002	0.0005
	R^2	0.9776	0.9987
Intra-particle diffusion	k_{id} (mg g ⁻¹ min ^{-1.5})	0.6591	0.4726
	C (mg g ⁻¹)	3.6838	9.7782
	R^2	0.8686	0.8328

composite is better described by the pseudo-second-order model than by the pseudo-first-order model. In addition, by looking at the calculated equilibrium adsorption capacity ($Q_{e1, cal}$ and $Q_{e2, cal}$), the resulting values from pseudo-second-order model were approximately closer to the experimentally obtained equilibrium adsorption capacity ($Q_{e, exp}$). These results indicate that the rate-determining step for adsorption of CV and MB by the prepared hydrogel may be a chemical sorption involving valence forces through sharing or exchange of electrons between adsorbent and sorbate [10, 24]. Among the mentioned models, the intra-particle diffusion model showed a poor fit to the experimental data, revealing that the intra-particle diffusion was not the rate-limiting step in the adsorption.

Effect of Initial Dye Concentration (Isotherm Studies)

The adsorption performance at different concentrations of dyes (20–200 mg L⁻¹), keeping all other parameters constant (GPAH4 = 20 mg, pH 7, time = 24 h) is presented in Fig. 7c.

The CV and MB adsorption percentage on GPAH4 nanocomposite decreases with the increase of the dye concentration. The adsorption percentage remained almost constant at 96% with the increase of the initial concentration of dyes up to 80 mg L⁻¹, and then started to decrease rapidly to less than 70% with further increase of the initial concentration up to 200 mg L⁻¹. These results suggest that there are plenty of adsorption sites in the GPAH4 nanocomposite which are occupied initially with the dye molecules and therefore the change of adsorption percentage was not obvious. At high concentration of dyes, a rapid decrease of adsorption percentage was observed due to the fact that the total existing adsorption sites on GPAH4 nanocomposite were filled with adsorbed dye molecules. As the weight of the adsorbent was kept constant, the number of existing adsorption sites on the hydrogel actually became the limiting factor that controlled the removal efficiency. However, the adsorption capacity of dyes increases rapidly with the increase of the dye concentration. The maximum adsorption capacity of CV and MB was determined as 169.6 and 173.2 mg g⁻¹, respectively.

The adsorption isotherms represent the interactive behavior of adsorbent and adsorbate at different initial dye concentrations and diagnose the mechanism of a particular adsorption process [25]. The most common adsorption isotherms models namely Langmuir and Freundlich were applied to study the equilibrium adsorption data of CV and MB on the prepared adsorbent. The Langmuir isotherm model (Eq. (8)) describes the equilibrium adsorption isotherms of homogeneous surfaces and it is utilized in monomolecular adsorption processes [26].

$$\frac{C_e}{Q_e} = \frac{C_e}{Q_m} + \frac{1}{K_L Q_m} \quad (8)$$

where Q_e (mg g⁻¹) and C_e (mg L⁻¹) are the adsorption capacity and the residual concentration of tested dyes in solution at equilibrium, respectively; Q_m (mg g⁻¹) and K_L (L mg⁻¹) are the amount of species adsorbed at complete monolayer coverage and a constant related to the affinity of the binding sites, respectively; Q_m and K_L can be determined from the linear plot of C_e/Q_e versus C_e .

Freundlich isotherm describes the adsorption on a heterogeneous surface, assuming that the stronger adsorption sites are occupied at first and the adsorption strength decreases with increasing the degree of adsorption site occupation [22]. It is mathematically described by Eq. (9).

$$\ln Q_e = \ln K_F + \frac{1}{n} \ln C_e \quad (9)$$

where K_F [(mg g⁻¹)(L mg⁻¹)^{1/n}] and n^{-1} are the Freundlich constants related to adsorption capacity and adsorption intensity. K_F and n can be determined from the linear plot of $\ln Q_e$ versus $\ln C_e$. On the basis of the n^{-1} value, the adsorption process can be classified as irreversible ($n^{-1}=0$), favorable ($0 < n^{-1} < 1$), or unfavorable ($n^{-1} > 1$).

The CV and MB adsorption isotherms for GPAH4 nanocomposite are presented in Fig. 8a, b. The calculated n^{-1} values are 0.2717 for MB and 0.2595 for CV dye adsorption and indicating the favorable adsorption of the dyes onto the GPAH4 nanocomposite. The adsorption of CV and MB by the GPAH4 nanocomposite strictly obeys the Langmuir isotherm equation, as shown by the plot of Q_e versus C_e (Fig. 8a, b) and the R^2 coefficients of 0.9672 for CV and 0.9706 for MB adsorption (Table 3). In addition, the theoretical monolayer capacities of GPAH4 nanocomposite ($Q_{m, cal}$ values) determined from the curve fittings are in good agreement with the $Q_{e, exp}$ values (Table 3). From the curve-fitting analysis based on the two isotherm models, it is concluded that the adsorption of the dyes onto the GPAH4 nanocomposite follows Langmuir-type model which implies the monolayer coverage of dyes.

Table 4 lists the comparison of the maximum CV or MB adsorption capacity (Q_m value) of the present adsorbent with some other adsorbents reported in the literature. This shows that the GPAH4 nanocomposite of the present study has relatively high adsorption capability compared with some other adsorbents [2, 19, 27–32].

Effect of Temperature (Thermodynamic Studies)

Thermodynamic studies are important to find out the nature of adsorption process. Figure 7d shows the relationship between the temperature and the adsorption percentage of CV and MB dyes by GPAH4 nanocomposite. As can be

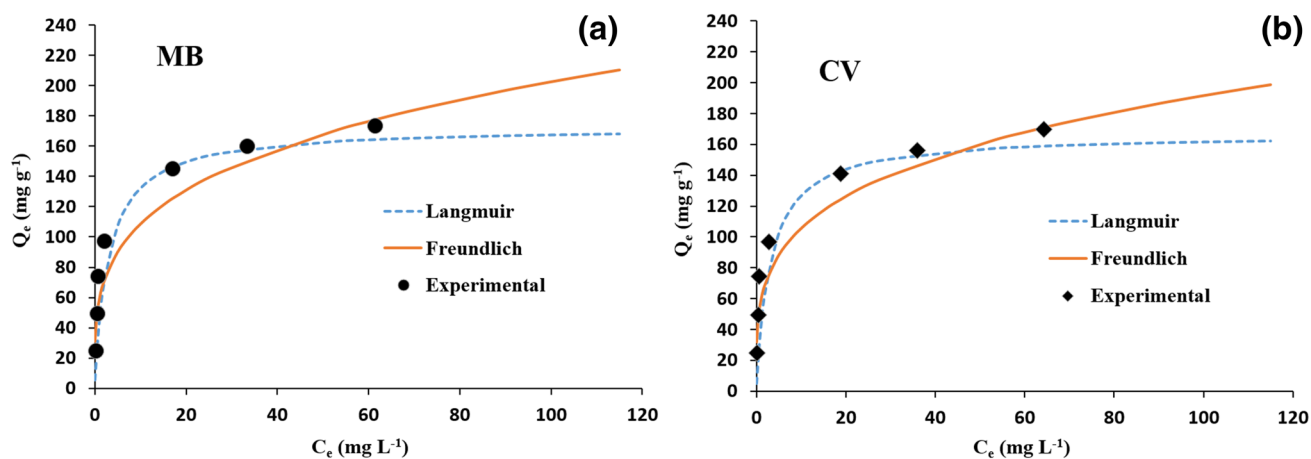


Fig. 8 a CV and b MB adsorption isotherms for GPAH4 nanocomposite

Table 3 Isotherm parameters for CV and MB sorption onto GPAH4 nanocomposite

Pollutants	$Q_{m,exp}$ (mg g^{-1})	Langmuir model			Freundlich model		
		$Q_{m,cal}$ (mg g^{-1})	K_L	R^2	K_F	n	R^2
CV	169.6	166.7	0.314	0.967	57.95	3.854	0.836
MB	173.2	172.4	0.324	0.971	57.98	3.680	0.826

Table 4 Comparison of CV and MB adsorption capacity on GPAH4 hydrogel with other adsorbents

Adsorbent	Q_m (mg g^{-1})		References
	CV	MB	
GPAH4 nanocomposite	169.6	173.2	This work
Starch-graft-poly(acrylic acid)	80.64	–	[2]
Treated ginger waste	64.93	–	[27]
Peanut shell carbon	146.84	–	[28]
Coniferous bark powder	32.78	–	[29]
Rice husk	–	40.5	[30]
Rice bran	42.25	–	[38]
NaOH modified rice husk (NMRH)	44.87	–	[35]
Konjacglucomannan /GO hydrogel	–	133.7	[19]
Pyrophyllite	–	70.42	[31]
Carbon nanotubes	–	35	[32]

seen, the adsorption percentage of the MB showed a slight rise with increasing the temperature from 25 to 55 °C, while the adsorption of CV showed the opposite trend with increasing temperature. The thermodynamic parameters including standard Gibbs free energy (ΔG^0), standard enthalpy change (ΔH^0), and standard entropy change (ΔS^0) were calculated according to the Eqs. (10) and (11), and can be used for estimation of the adsorption process.

$$\Delta G_0 = -RT \ln K_L \quad (10)$$

$$\ln K_L = -\frac{\Delta H_0}{RT} + \frac{\sum S_0}{R} \quad (11)$$

where K_L is the ratio of concentration of CV or MB adsorbed by the adsorbent (Q_e) to their remaining concentration in solution at equilibrium (C_e). The slope and intercept of the plot of $\ln K_L$ versus $1/T$ give ΔH^0 and ΔS^0 respectively, and the obtained data are listed in Table 5.

The negative value of ΔG^0 suggests that the adsorption of CV and MB dyes on the GPAH4 nanocomposite is

Table 5 Thermodynamic parameters for adsorption of CV and MB onto GPAH4 nanocomposite

Pollutants	ΔH^0 (KJ mol^{-1})	ΔS^0 ($\text{J mol}^{-1} \text{K}^{-1}$)	$-\Delta G^0$ (KJ mol^{-1})			
			25 °C	35 °C	45 °C	55 °C
CV	–63.11	–172.9	11.61	9.58	8.52	6.19
MB	73.3	283.4	11.16	14.03	16.80	19.6

thermodynamically feasible and spontaneous in nature. The ΔG^0 values of MB adsorption onto GPAH4 nanocomposite decreased with an increase in temperature indicating an increased trend in the degree of spontaneity and feasibility of adsorption. The positive value of ΔH^0 confirmed the endothermic nature of the MB dye sorption process. The positive value of ΔS^0 suggested an increased randomness at the solid/solution interface occurs in the internal structure of the adsorption of MB onto GPAH4 nanocomposite. Similar trend of adsorption was observed in some literatures [33, 34]. However, the ΔG^0 values for CV dye adsorption increased as the temperature increased suggesting that CV adsorption was less favorable at higher temperatures. The enthalpy (ΔH^0) and entropy (ΔS^0) changes estimated from the slope and the intercept of plots for Eq. (11) was $-63.11 \text{ kJ mol}^{-1}$ and $-172.9 \text{ J mol}^{-1} \text{ K}^{-1}$ respectively. The negative value of ΔH^0 is indicative of the fact that adsorption of CV by GPAH4 nanocomposite is controlled by an exothermic process. The negative value of ΔS^0 suggests that the process is enthalpy driven [35]. Similar trend has also been observed for adsorption of CV by eggshells [36] and coniferous pinus bark powder [29]. The different trend in adsorption of CV and MB molecules can be due to the configuration of their molecules and the way these molecules make contact with the surface functional groups of adsorbent (Fig. 9). It is

proposed that CV molecules have weaker interaction with active sites rather than MB molecules because of their probable oblique configuration [37]. As the temperature increases, the oblique orientation decreases the area of close contact and also strengthens the interaction between the adsorbed CV molecules themselves. As a result, the CV is more difficult to be adsorbed at high temperature. However, the MB molecules interact strongly with the adsorbent due to having parallel configuration with the adsorbent surface. As the temperature increases, MB molecules dissociate from each other and form stronger interaction with the adsorbent functional groups.

The photos taken after adsorption of CV and MB by the adsorbent GPAH4 at different temperatures are shown in Fig. 10 (the adsorbent was removed by filtration). As can be seen, the MB was adsorbed more by the adsorbent as the temperature increased from 25 to 55 °C. The CV dye was adsorbed more by the adsorbent at 25 °C and the adsorption percentage decreased as the temperature increased to 55 °C.

Regeneration of GPAH4 Hydrogel Nanocomposite

To regenerate and reuse the adsorbent, the MB and CV dyes adsorbed on the GPAH4 hydrogel were desorbed by NaOH solution and ethanol respectively. Desorption of CV and MB from GPAH4 hydrogel was shown in Fig. 11. The adsorption

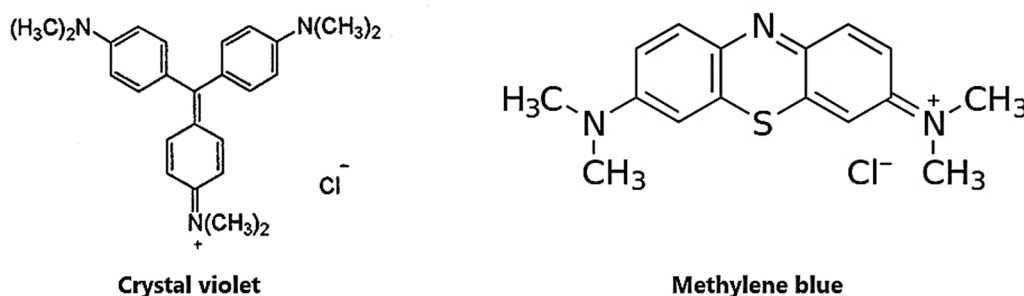


Fig. 9 Chemical structure of CV and MB

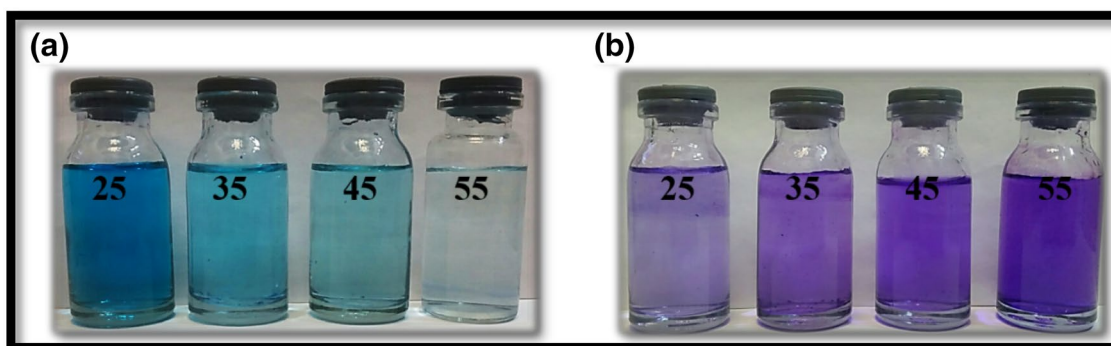


Fig. 10 Color changes of **a** MB and **b** CV solutions using GPAH4 adsorbent at different temperatures

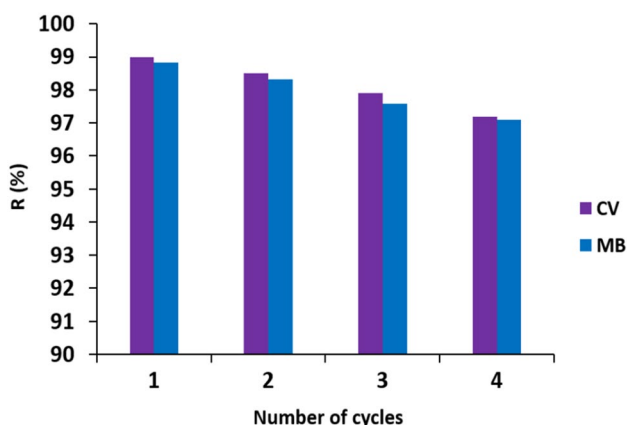


Fig. 11 Desorption of CV and MB from GPAH4 hydrogels

of the GPAH4 hydrogel nanocomposite for both MB and CV dyes could still exceed 97% in the 4th cycle which is slightly lower than the first adsorption. It means that regeneration efficiency of the GPAH4 hydrogel nanocomposite is still high, and it can be well recovered as adsorbents for MB and CV dyes, leading to the fact that GPAH4 hydrogel nanocomposite has a good potential as reusable adsorbents of dyes from wastewater for commercial applications.

Conclusion

In this study, we demonstrated a facile two-step approach to prepare pH sensitive PVA-based hydrogel nanocomposites (GPAH1-4). These hydrogels were characterized and used as adsorbent for removal of typical cationic dyes (Crystal violet and methylene blue) from aqueous solution. The results showed that the adsorbent dosage, pH, initial concentration, contact time, and temperature played a significant role in the dye adsorption capacity of GPAH4. Kinetic experiments showed that the adsorption process followed pseudo-second-order kinetic model. Adsorption isotherm study indicated that the adsorption of MB and CV dyes on the adsorbent was a monolayer adsorption, and the maximum adsorption capacity was estimated to be 173.2 and 169.6 mg g⁻¹. According to the thermodynamic study, enthalpy of CV adsorption is exothermic while that of MB is endothermic. The different adsorption trend for CV and MB onto GPAH4 was observed by increase of temperature due to the differences in the pattern of adsorption.

References

- Gupta V (2009) *J Environ Manage* 90:2313
- Pourjavadi A, Hosseini SH, Seidi F, Soleyman R (2013) *Polym Int* 62:1038

- Kunz A, Mansilla H, Duran N (2002) *Environ Technol* 23:911
- Shen C, Song S, Zang L, Kang X, Wen Y, Liu W, Fu L (2010) *J Hazard Mater* 177:560
- Wu H, Wang S, Kong H, Liu T, Xia M (2007) *Bioresour Technol* 98:1501
- Gupta VK, Jain R, Varshney SJ (2007) *Colloid Interface Sci* 312:292
- Roufegari-Nejhad E, Sirousazar M, Abbasi-Chiyaneh M, Kheiri F (2019) *J Polym Environ* 27:2239
- Li S, Liu X (2008) *Polym Adv Technol* 19:371
- Taleb MFA, El-Mohdy HA, El-Rehim HA (2009) *J Hazard Mater* 168:68–75
- Sekhavat Pour Z, Ghaemy M (2015) *RSC Adv* 5:64106
- Sekhavat Pour Z, Makvandi P, Ghaemy M (2015) *Int J Biol Macromol* 80:596
- Sun L, Fugetsu B (2014) *Chem Eng J* 240:565
- Sahraei R, Sekhvat Pour Z, Ghaemy M (2016) *J Clean Prod* 142:2973
- Sahraei R, Ghaemy M (2017) *Carbohydr Polym* 157:823
- Liu H, Wu J, Liu C, Pan B, Kim NH, Lee JH (2018) *Compos B* 155:391
- Liu C, Liu H, Zhang K, Dou M, Pan B, He X, Lu C (2019) *Bioresour Technol* 282:148
- Huang Y, Zeng M, Ren J, Wang J, Fan L, Xu Q (2012) *Colloid Surf A* 401:97
- Wan YJ, Tang LC, Gong LX, Yan D, Li YB, Wu LB, Jiang JX, Lai GQ (2014) *Carbon* 69:467
- Gan L, Shang S, Hu E, Yuen CWM, Jiang SX (2015) *Appl Surf Sci* 357:866
- Dotto G, Pinto L (2011) *Carbohydr Polym* 84:231
- Hosseinzadeh H, Zoroufi S, Mahdavinia GR (2015) *Polym Bull* 72:1339
- Sun XF, Liu B, Jing Z, Wang H (2015) *Carbohydr Polym* 118:16
- SekhavatPour Z, Ghaemy M (2016) *Polym Adv Technol* 12(57):1557–1568
- Peng Q, Liu M, Zheng J, Zhou C (2015) *Microporous Mesoporous Mater* 201:190
- Fosso-Kankeu E, Mittal H, Mishra SB, Mishra AK (2015) *J Ind Eng Chem* 22:171
- Wang J, Wei L, Ma Y, Li K, Li M, Yu Y, Wang L, Qiu H (2013) *Carbohydr Polym* 98:736
- Kumar R, Ahmad R (2011) *Desalination* 265:112
- Zhang J, Ou L (2013) *Water Sci Technol* 67:737
- Ahmad RJ (2009) *Hazard Mater* 171:767
- Vadivelan V, Kumar KV (2005) *J Colloid Interface Sci* 286:90
- Gücek A, Şener S, Bilgen S, Mazmanci MA (2005) *J Colloid Interface Sci* 286:53
- Yao Y, Xu F, Chen M, Xu Z, Zhu Z (2010) *Bioresour Technol* 101:3040
- Rahchamani J, Mousavi HZ, Behzad M (2011) *Desalination* 267:256
- Ghorai S, Sarkar AK, Panda AB, Pal S (2013) *Bioresour Technol* 144:485
- Chakraborty S, Chowdhury S, Saha PD (2011) *Carbohydr Polym* 86:1533
- Chowdhury S, Chakraborty S, Saha PD (2013) *Waste Biomass Valoriz* 4:655
- Rytwo G, Ruiz-Hitzky E, Therm J (2003) *Anal Calorim* 71:751
- Wang XS, Liu X, Wen L, Zhou Y, Jiang Y, Li Z (2008) *Separ Sci Technol* 43:3712

Publisher's Note Springer Nature remains neutral with regard to jurisdictional claims in published maps and institutional affiliations.

Affiliations

Mina Rabipour¹ · Zahra Sekhvat Pour¹ · Razieh Sahraei² · Mousa Ghaemy¹ · Mehdi Erfani Jazi³ · Todd E. Mlsna³

✉ Zahra Sekhvat Pour
zsekhvat@gmail.com

¹ Polymer Research Laboratory, Faculty of Chemistry,
University of Mazandaran, Babolsar, Iran

² Department of Polymer Engineering, Amirkabir University
of Technology (Tehran Polytechnic), Hafez Ave., P.O. Box:
15875-4413, Tehran, Iran

³ Department of Chemistry, Mississippi State University,
Mississippi State, MS 39762, USA